RSC Advances

PAPER

View Article Online
View Journal | View Issue

Cite this: *RSC Adv.*, 2023, **13**, 30990

Gamma radiation effects on AG MP-50 cation exchange resin and sulfonated activated carbon for bismuth-213 separation†

Hongshan Zhu,[abc] Stephan Heinitz,[a] Samuel Eyley,[d] Wim Thielemans,[d] Elien Derveaux,[e] Peter Adriaensens,[e] Koen Binnemans,[b] Steven Mullens[c] and Thomas Cardinaels *[ab]

Medical $^{225}Ac/^{213}Bi$ radionuclide generators are designed to provide a local supply of the short-lived ^{213}Bi for cancer treatment. However, radiation-induced damage to the sorbents commonly used in such radionuclide generators remains a major concern. In this study, the effects of gamma radiation on AG MP-50 cation exchange resin and sulfonated activated carbon (SAC) were studied by analyzing the changes in the morphological characteristics, functional groups, and the La^{3+}/Bi^{3+} sorption performance, with La^{3+} being a suitable non-radioactive substitute for Ac^{3+}. The surface sulfonic acid groups of AG MP-50 resin suffered from severe radiation-induced degradation, while the particle morphology was changed markedly after being exposed to absorbed doses of approximately 11 MGy. As a result, the sorption performance of irradiated AG MP-50 for La^{3+} and Bi^{3+} was significantly decreased with increasing absorbed doses. In contrast, no apparent changes in acquired morphological characteristics were observed for pristine and irradiated SAC based on SEM and XRD characterization. The surface oxygen content (*e.g.*, O–C=O) of irradiated SAC increased for an absorbed dose of 11 MGy due to free radical-induced oxidation. The sorption performance of pristine and irradiated SAC materials for La^{3+} and Bi^{3+} remained generally the same at pH values of 1 and 2. Furthermore, the applicability of AG MP-50 and SAC in the $^{225}Ac/^{213}Bi$ generators was illustrated in terms of their radiolytic stability. This study provides further evidence for the practical implementation of both AG MP-50 and SAC in $^{225}Ac/^{213}Bi$ radionuclide generators.

Received 8th September 2023
Accepted 16th October 2023

DOI: 10.1039/d3ra06130b

rsc.li/rsc-advances

1. Introduction

The use of $^{225}Ac/^{213}Bi$ radionuclide generators is receiving considerable interest for the production and separation of ^{213}Bi, which is regarded as a promising radionuclide that can be applied in the treatment of various types of cancers (*e.g.*, prostate cancer, bladder carcinoma, and leukemia).[1–3] Typically, $^{225}Ac/^{213}Bi$ generators are classified based on the sorption affinity of the sorbents used for the radionuclide of interest.[1,4–6] For the direct generator, the sorbent has the ability to adsorb both ^{225}Ac and ^{213}Bi radionuclides, whereas ^{213}Bi can be selectively eluted at specified time intervals.[4,5] In contrast, the sorbents in an inverse generator system are only selective towards ^{213}Bi, which can be eluted in the following stage.[6]

A typical radionuclide generator is expected to be loaded with at least 4 GBq of ^{225}Ac on demand.[7] When designing sorbents for the separation of elevated activities of ^{213}Bi, radiation-induced damage resulting from their exposure to intense radioactivity should be considered.[1,8,9] ^{225}Ac is a relatively long-lived and highly cytotoxic radionuclide ($t_{1/2}$ = 9.920 days). Its decay pathway primarily involves a sequence of four alpha decays and two beta disintegrations ending with quasi-stable ^{209}Bi, as shown in Fig. 1.[5,10,11] Most of the intermediates in the decay path have high energies, *e.g.*, significant radiation of 5.9–8.4 MeV for the alpha emitters and 0.6–2.0 MeV for the beta emitters.[5,10,11] Additionally, a series of gamma photons are produced with the two most dominant emissions originating from the disintegration of ^{221}Fr (218 keV, 11.6% emission probability) and ^{213}Bi (440 keV, 26.1% emission probability).[5,10,11] The most challenging radiation in terms of shielding comes from the gamma photon emissions by ^{209}Tl decay, originating from the 2.09% alpha branch of ^{213}Bi.[12]

[a]*Belgian Nuclear Research Centre (SCK CEN), Institute for Nuclear Materials Science, Boeretang 200, Mol, B-2400, Belgium. E-mail: thomas.cardinaels@sckcen.be*

[b]*Department of Chemistry, KU Leuven, Celestijnenlaan 200F, P. O. 2404, B-3001 Leuven, Belgium*

[c]*Flemish Institute for Technological Research (VITO NV), Sustainable Materials Management, Boeretang 200, Mol, 2400, Belgium*

[d]*Department of Chemical Engineering, Sustainable Materials Lab, KU Leuven, Campus Kulak Kortrijk, Etienne Sabbelaan 53, Kortrijk 8500, Belgium*

[e]*Universiteit Hasselt, Analytical & Circular Chemistry, Campus Diepenbeek, Agoralaan Gebouw D, B-3590, Diepenbeek, Belgium*

† Electronic supplementary information (ESI) available. See DOI: https://doi.org/10.1039/d3ra06130b

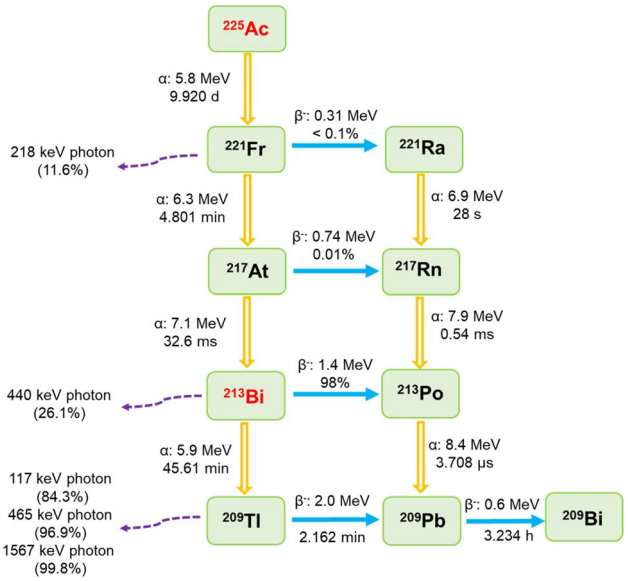

Fig. 1 Decay scheme of ^{225}Ac.[5,10,11]

The impact of radiation damage on a material is determined by a combination of the absorbed dose, the type of radiation, the dose rate, and the irradiation atmosphere.[13] The underlying mechanisms of radiolysis of ion exchange resins include the decomposition and scission of the functional groups, modification of the degree of cross-linking, and possible interactions of the resin with degradation products like sulfonic acid.[13,14] These effects can lead to considerable changes in material characteristics, and consequently to the separation performance towards isotopes of interest.[8,9,14,15] Hence, it is essential to understand more specifically the radiolytic effects on the material properties and the sorbent performance in ^{225}Ac/^{213}Bi separation.

Several material classes have been investigated as sorbents for ^{225}Ac/^{213}Bi generators. For direct generators, AG MP-50, being a macroporous resin composed of sulfonic acid groups bonded to a styrene-divinylbenzene matrix, is a commonly used strong acid cation exchanger.[16] For inverse generators, UTEVA resin (dipentyl pentylphosphonate sorbed onto an inert support) demonstrated Bi^{3+} sorption in an HCl medium, linked to the presence of negatively charged $BiCl_4^-$ species.[5,6] In addition, AG MP-50 resin and its analogs (*e.g.*, AG 50W-X8) can also be utilized in the guard or accumulation (second) column to improve the purity and concentration of ^{213}Bi.[2,6,17] However, as has been previously reported in the literature, such types of materials are susceptible to ionizing irradiation.[4,8,9,14,15] Previous research showed that exposure to gamma radiation leads to the formation of carboxylic and phenolic functional groups in AG MP-50.[18] However, as the sorption is mainly governed by the strongly acidic sulfonic acid groups, these weaker acidic groups are likely to impact the sorption performance.[18] Furthermore, the presence of these oxygen-containing groups could negatively affect the ^{213}Bi yield due to their strong sorption affinity towards ^{213}Bi.[19] To examine the changes in the sulfonic acid functional groups of AG MP-50 after irradiation, a relatively high acidic matrix should be chosen to study the exchange/sorption capacity for ^{225}Ac, which would ignore the contribution of the other acidic functional groups.[20] This is due to the low pK_a value of the sulfonic acid groups and the high pK_a value for the carboxylic and phenolic groups.[20] Accordingly, an insightful analysis of the sorption of ^{225}Ac (or its surrogates) onto irradiated AG MP-50 is of utmost importance. In addition, to the best of our knowledge, there are no reports available that describe the morphology changes of both pristine and irradiated AG MP-50 using SEM techniques. Therefore, further investigations are needed to study the radiolytic stability of AG MP-50.

In inverse generator systems, which aim to reduce the inflicted radiation dose towards the resin, radiolysis does also occur.[4] It was reported that the sorption capacity of irradiated UTEVA for ^{213}Bi decreased significantly with increasing absorbed dose.[4] Hence, alternative materials with high radiolytic stability for UTEVA are required. In our earlier work, sulfonated activated carbon material (SAC) was evaluated as a potential alternative sorbent for application in inverse ^{225}Ac/^{213}Bi generators.[19] It was demonstrated that ^{225}Ac selectively adsorbed onto the sulfonated activated carbon over ^{213}Bi by adjusting the sorption conditions, including the salt concentration and pH value. Concerning the radiolytic stability, the sulfonated activated carbon showed equal La^{3+} and Bi^{3+} sorption capacities after receiving an absorbed dose of 1 MGy of gamma radiation (both in wet and dry conditions). However, no full material characterization was performed to fully understand the material changes at higher absorbed doses (>1 MGy).[19] These investigations are essential for further evaluating these sorbent materials for the targeted application.

This work aimed to examine the gamma radiation stability of AG MP-50 resin and sulfonated activated carbon material, as shown in Fig. 2. Gamma rays can have a uniform effect on materials with large bulk structures and high porosity due to the high penetration range that they exhibit.[21] Furthermore, compared to alpha and beta irradiation, gamma irradiation can be carried out without the risk of contaminating the irradiated materials.[4,22,23] It should be noted, however, that alpha irradiation typically causes larger damage to the sorbents compared to gamma irradiation.[4,22,23] As previously reported, the decrease in sorption capacity of Dowex 50W-X4 (an analog of AG MP-50) towards yttrium was larger after exposure to alpha radiation compared to the same dose of gamma radiation.[4,22,23] The radiation-induced damage could be primarily due to the ionizing radiation absorbed by the sorbents (direct effects) or reactions between radiolysis products in solution and the sorbents (indirect effects).[24] There might be no significant difference in the indirect effects of either alpha or gamma irradiation, as opposed to direct effects.[22] While gamma irradiation may not fully reflect the real situation of ^{225}Ac irradiation, the findings presented in this study can provide essential preliminary information for further research. Moreover, this research can also yield useful insights for other fields, such as surface modifications of materials by gamma irradiation.[25,26]

Herein, AG MP-50 and SAC materials were exposed to a ^{60}Co gamma source to an absorbed dose between 0–11 MGy under

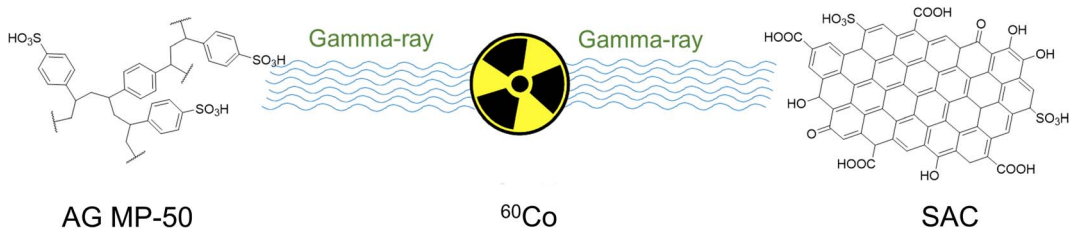

Fig. 2 Structure of AG MP-50 and SAC.

wet conditions in 1 mol L^{-1} HCl. The selection of a 1 mol L^{-1} HCl solution in this study aimed to enable a comparison with previously used materials under the same irradiation liquid phase, as discussed in a review paper.[4] Additionally, AG MP-50 was expected to be employed for the further purification of ^{213}Bi eluate in 1 mol L^{-1} HCl, derived from an inverse generator.[27] The impact of the radiation on the material characteristics for AG MP-50 and SAC was then examined by carrying out scanning electron microscopy (SEM) and X-ray diffraction (XRD) measurements. The identification and quantification of the chemical structures of these materials were determined by diffuse reflectance infrared Fourier transformations (DRIFT), solid-state nuclear magnetic resonance (NMR), and X-ray photoelectron spectroscopy (XPS). Batch sorption tests were performed to evaluate their sorption performance towards La^{3+} (a substitute for Ac^{3+}) and Bi^{3+}. Finally, the application of these materials in the direct/inverse $^{225}Ac/^{213}Bi$ generators was described from the perspective of their radiolytic stability.

2. Experimental

2.1. Material and reagents

$La(NO_3)_3 \cdot 6H_2O$ (99.99%), $Bi(NO_3)_3 \cdot 5H_2O$ (98%), H_2SO_4 (95.0–98.0%), and HNO_3 (>65%) were supplied by Sigma-Aldrich. HCl (37%) was supplied by Thermo Fisher Scientific. Milli-Q water (18.2 MΩ·cm 25 °C) was used in the experiments. Briefly, activated carbon Norit CA1 was purchased from Sigma-Aldrich and then underwent a sulfonation process (15 g of Norit CA1 into 150 mL concentrated H_2SO_4) under 150 °C for 3 hours, as described in our earlier work (the SAC is named SNCA-150 in our earlier work).[19] AG MP-50 resin was purchased from Bio-Rad Laboratories. No further purification was performed on these materials and reagents.

2.2. Gamma irradiation experiments

The prepared AG MP-50 and SAC samples were irradiated by a ^{60}Co source in a glass vial under wet conditions.[28] The dosimetry and methodology from our institution have been described elsewhere.[28] We present a brief introduction of the gamma irradiation experiment in the following: 200 mg of AG MP-50 or SAC was mixed with 2 mL of 1 mol L^{-1} HCl solution in a glass vial and then irradiated by ^{60}Co. The absorbed dose for AG MP-50 or SAC was in the range of 0.5 to 11 MGy, and the dose rate was controlled to approximately 7–10 kGy h^{-1} (effect of position within BRIGITTE). The error in the received doses was less than 10%. Finally, the samples were washed and dried in an oven at a temperature value of 70 °C. The employed irradiation conditions are presented in Table 1.

2.3. Characterizations

Scanning electron microscopy (SEM, FEI Nova NanoSEM 450) was used to characterize the morphology and particle sizes of the samples. X-ray diffraction (XRD, X'Pert Pro, Cu-tube) was

Table 1 Gamma-ray irradiation conditions and the surface equivalent homogeneous elemental composition of the pristine and irradiated AG MP-50 and SAC[a]

	Gamma-ray irradiation conditions			Equivalent homogeneous composition			
Sample	Dose rate (kGy h^{-1})	Received dose (MGy)	Deviation (%)	C (at%)	O (at%)	S (at%)	C 1s O–C=O (at%)
AG MP-50	0	0	0	71.6 ± 0.1	21.7 ± 0.3	6.5 ± 0.4	0.9 ± 0.7
	9.5	0.5	2	nm	nm	nm	nm
	6.9	1.0	2	71.0 ± 0.1	22.3 ± 0.1	6.4 ± 0.1	0.7 ± 0.1
	7.4	1.5	5	nm	nm	nm	nm
	8.0	2.0	2	nm	nm	nm	nm
	8.4	11	10	74.2 ± 0.3	20.5 ± 0.4	4.5 ± 0.1	2.3 ± 0.5
SAC	0[b]	0	0	84.3 ± 0.2	14.3 ± 0.1	0.9 ± 0.1	2.7 ± 0.1
	10.1	0.5	4	nm	nm	nm	nm
	7.3	1.0	4	84.7 ± 0.2	14.3 ± 0.3	0.5 ± 0.1	3.2 ± 0.1
	7.4	1.5	5	nm	nm	nm	nm
	7.9	2.0	1	nm	nm	nm	nm
	8.3	11	10	81.4 ± 0.1	17.4 ± 0.1	0.5 ± 0.1	4.5 ± 0.2

[a] nm (not measured). [b] Data from our earlier work.[19]

used to investigate the structures of the pristine and irradiated samples. The species of functional groups and their quantitative analysis were determined by X-ray photoelectron spectroscopy (Kratos Axis Supra spectrometer, with monochromatic Al monochromatic X-ray source, full details in ESI†) and Fourier-transform infrared spectroscopy (FT-IR, Nicolet 6700) with an *in situ* DRIFT accessory type 'Harrick Praying Mantis'. Detailed information on the above characterization methods can be found in our earlier work.[27]

Solid state ^{13}C-CPMAS (Cross Polarization Magic Angle Spinning) NMR spectra were acquired on a Jeol ECZ600R 600 MHz spectrometer (14.1 Tesla) equipped with a 3.2 mm wide VT Range HXMAS probe. MAS was performed at 20 kHz. The aromatic signal of hexamethylbenzene was used to calibrate the carbon chemical shift scale (132.1 ppm). Acquisition parameters used for the CPMAS measurements were: a spectral width of 85 kHz, a 90° pulse length of 2.24 μs, a spin-lock field for CP of 70 kHz, a contact time of 1.0 ms, an acquisition time of 12 ms, a recycle delay time of 3 s, and between 55 000 and 80 000 scans (for the AG MP-50 samples) and between 60 000 and 112 000 scans (for the SAC samples). High-power proton dipolar decoupling during acquisition was set to 80 kHz.

2.4. Batch sorption experiments

Ten milligram of sorbent was initially placed in 15 mL plastic centrifuge tubes and then mixed with 10 mL of the liquid phase, which included 10 μmol L^{-1} La^{3+} and 10 μmol L^{-1} Bi^{3+}. The pH of the liquid phase for non-irradiated and irradiated SAC was adjusted to pH = 1 and pH = 2. A detailed sorption process can be found in our previous work.[19] The HNO_3 concentration for non-irradiated and irradiated AG MP-50 was 1.5 mol L^{-1}. The mixture was shaken at 120 rpm for 24 h. The solid and liquid phases were separated using 0.45 μm PTFE syringe filters, and then the concentrations of La^{3+} and Bi^{3+} were measured by Thermo X-Series II quadrupole ICP-MS.

2.5. Equations for calculation

The removal percentage R (%) and distribution coefficient K_d (mL g^{-1}) are as follows:

$$R\ (\%) = \frac{C_0 - C_e}{C_0} \times 100\% \quad (1)$$

$$K_d = \frac{C_0 - C_e}{C_e} \times \frac{V}{m} \quad (2)$$

where m (g) and V (mL) represent the mass of the sorbent and the volume of the liquid, respectively. C_0 (μmol L^{-1}) and C_e (μmol L^{-1}) refer to the initial and equilibrium concentrations of La^{3+} or Bi^{3+}, respectively.

3. Results and discussion

3.1. Effect of gamma irradiation on morphological changes

The macroscopic appearance of both AG MP-50 and SAC, before and after exposure to gamma radiation towards an absorbed dose in the range of 0.5 to 11 MGy, is displayed in Fig. 3. The pristine and irradiated AG MP-50 resins underwent a color change from light to dark amber and then to dark red with increasing absorbed dose (Fig. 3a). More specifically, the darker appearance of AG MP-50 irradiated to an adsorbed dose of 11 MGy was clearly visible in comparison to that of the AG MP-50 resins irradiated to lower doses. It was also reported in the literature that the darkening for organic ion exchange resins was a result of high exposure to ionizing radiation.[8,9,29] Furthermore, this phenomenon was usually accompanied by the manifestation of the gouging, pitting, cracking, and peeling in such types of polymer resin particles.[8,9,30] These outcomes clearly indicate that the irradiated AG MP-50 structure suffered from high levels of radiation-induced damage, especially at an absorbed dose of 11 MGy. A more detailed view on the change of the microstructure is obtained by SEM analysis (Fig. 4a–d and S1a–d†). Pristine AG MP-50 exhibited an irregular shape with a particle size of approximately 75–150 μm. The radiolytic impact on particle size and shape was not obviously evident at an absorbed dose of 0–2 MGy, while the aggregation of particles was observed for the sample that received a dose of 11 MGy. Moreover, the size of the aggregated particles increased as the absorbed dose increased. However, the size of the small particles that formed large aggregate particles slightly decreased (Fig. 4c and d), possibly due to radiolytic decomposition of the polymeric chains.[31] The particle aggregation behavior could be attributed to the degradation of the polymeric structures and radiation-induced free radical polymerization.[32] Therefore, these results demonstrate that the AG MP-50 particles were highly sensitive to ionizing radiation in the absorbed dose range reported herein. In addition, in the acquired XRD

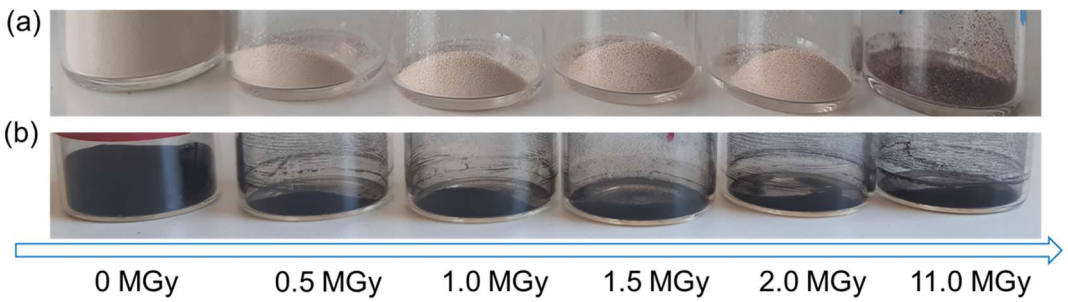

Fig. 3 Pictures of AG MP-50 (a) and SAC (b) before and after exposure to gamma radiation.

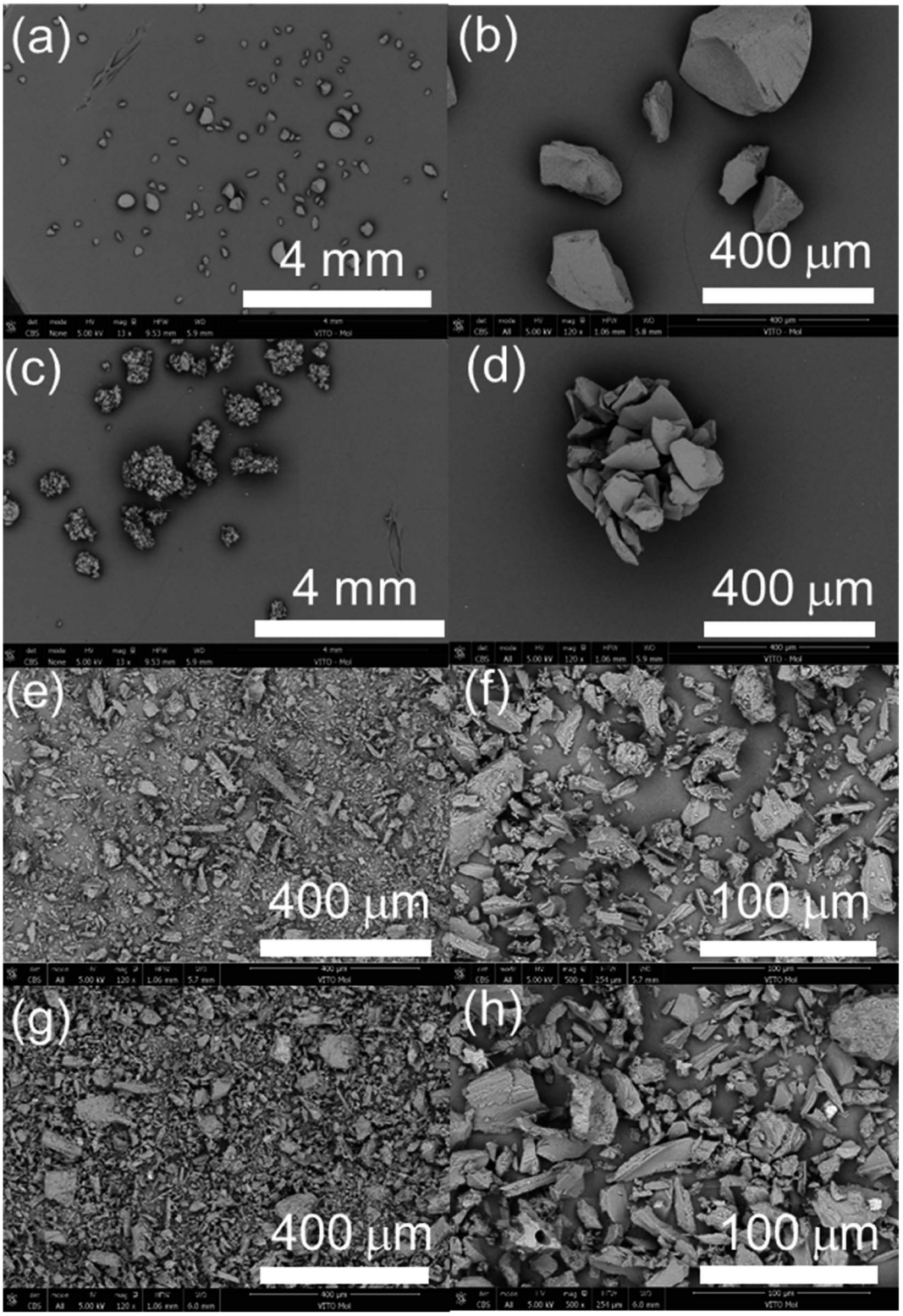

Fig. 4 SEM images of AG MP-50 (0 MGy (a and b), and 11 MGy (c and d)) and SAC (0 MGy (e and f), and 11 MGy (g and h)) before and after exposure to gamma radiation.

patterns (Fig. 5a), the broad peak at ~17° is attributed to the amorphous structure of AG MP-50 matrix, a characteristic typically seen in other polymers.[33] There are no obvious differences between the pristine and irradiated materials, possibly due to the high penetration range of XRD technique and the amorphous structure being preserved.

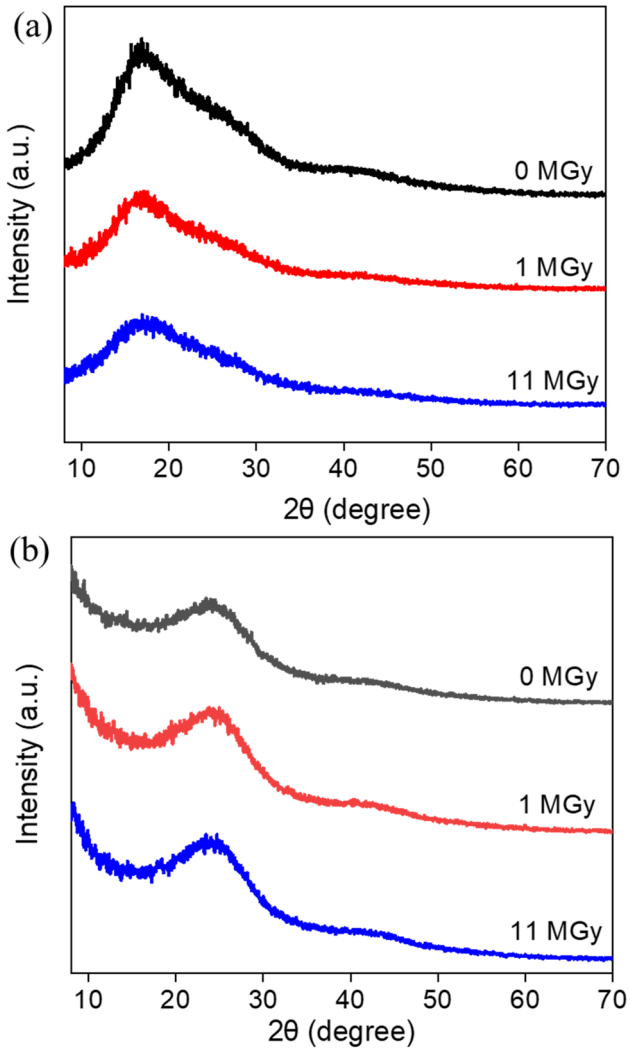

Fig. 5 XRD patterns of the pristine and irradiated AG MP-50 (a) and SAC (b) materials.

No noticeable color change (Fig. 3b) was observed for irradiated SAC in relation to pristine SAC. This phenomenon could also be attributed to its inherently dark initial color. As displayed in Fig. 4e and f, the acquired SEM images demonstrate that the pristine SAC was composed of an irregularly shaped precursor powder, ranging from a few micrometers to several tens of micrometers. No obvious impact on the morphology and particle sizes of SAC (Fig. 4g, h, S1e and h†) after receiving high doses (1–11 MGy) could be observed. Fig. 5b depicts the XRD patterns of the pristine and irradiated SAC materials. The broad peak at approximately $2\theta = 15°–30°$ corresponds to the (002) plane, suggesting that carbon materials consisting of aromatic carbon sheets were oriented randomly.[34] Using $2\theta = 24.1°–24.2°$ as peak value for the pristine and irradiated SAC materials, d_{002} (nm) was calculated to be 0.37 nm using the Bragg equation ($n\lambda = 2d \sin\theta$).[35,36] No apparent changes were observed in the collected XRD patterns of the SAC materials exposed to gamma radiation. Based on the SEM and XRD analysis, it is concluded that the structure of SACs was not sensitive to gamma radiation, or at least no evidence of any change was detected.

3.2. Effect of gamma irradiation on chemical structure

Apart from the impact on the morphology, radiolytic effects can also be expected on the chemical structure itself. Therefore, a combination of analytical tools is used to map the main characteristics of the materials as a function of the absorbed dose. Especially, the degradation of the existing functional groups, or the formation of other groups on the surface are relevant to the sorption performance. Table 1 presents the surface elemental composition of the pristine and irradiated AG MP-50 and SAC from the XPS quantitative data, and the detailed XPS analysis results can be found in the ESI (Tables S1–S4, Fig. S2 and S3).†

3.2.1. AG MP-50 resin. Fig. 6a presents the DRIFT spectra of AG MP-50 resin before and after irradiation up to absorbed doses of 1 and 11 MGy. Apart from the peaks related to the styrene-divinylbenzene copolymer backbone, characteristic peaks in DRIFT spectra can be attributed to the stretching vibration of sulfonic acid groups (1173, 1125, 1026, 1001, and 672 cm^{-1}).[4,37] In addition, two DRIFT bands at approximately

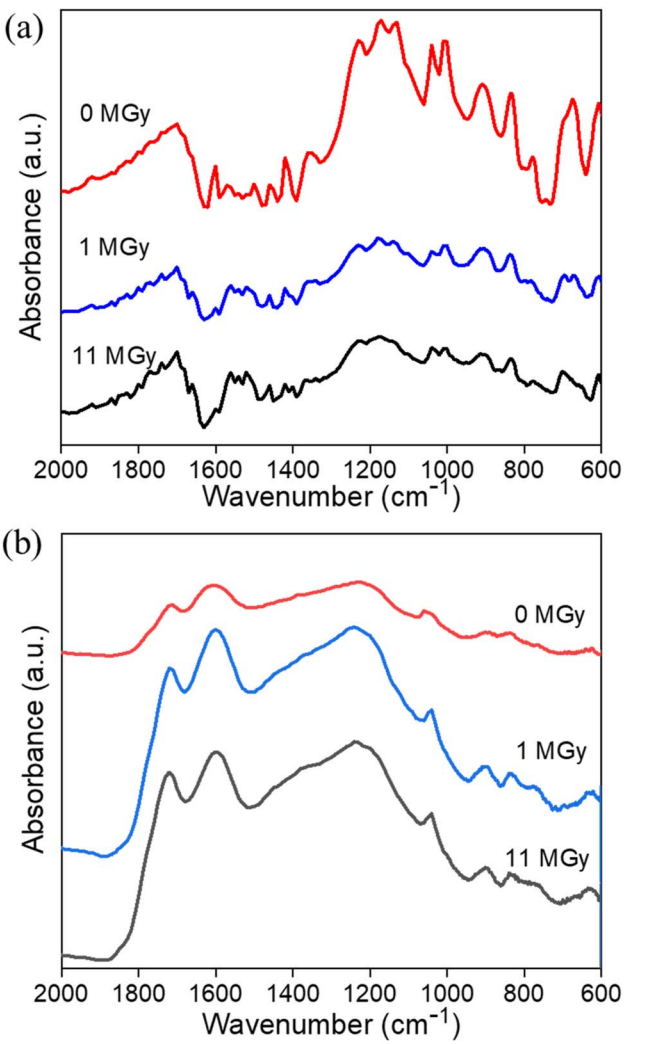

Fig. 6 DRIFT spectra of the pristine and irradiated AG MP-50 (a) and SAC (b).

905 and 831 cm^{-1} were assigned to the C–H bond out-of-plane bending in the benzene rings, while the band at 1413 cm^{-1} was attributed to the in-plane vibration of the C=C bond.[37] With increasing absorbed doses up to 11 MGy, no obvious change in the DRIFT spectra was observed, apart from a decrease in absorbance intensity, probably related to the darkening of the samples as discussed earlier. More information on the structural changes was obtained from the NMR spectra (Fig. 7a) and high-resolution XPS analysis (Fig. 8a–c) of the pristine and irradiated AG MP-50 resins. The presence of sp^3 carbon atoms was demonstrated by the presence of a signal around 42 ppm (parts per million) in the NMR spectra. However, its signal intensity decreased with irradiation dose, indicating the degradation of aliphatic structures by gamma irradiation. The intense peak at around 127 ppm and the weaker peak at around 140 ppm arise from carbon atoms in aromatic rings (sp^2 carbons) without heteroatoms attached.[38] It is clear that the intensity of the latter peak (at 148 ppm) increases upon increasing the irradiation dose. Also the signal intensity around 148 ppm, typically for aromatic carbons with OH/OR groups attached, increased upon increasing the absorption dose. This points to oxidation of the AG MP-50 structure. The XPS C 1s spectra were dominated by C=C/C–C bands. These results are relevant to the styrene-divinylbenzene copolymer lattices. As the absorbed dose increased, one additional peak (at 289 eV) and a broadening of the shoulder (286–288 eV) emerged in the C 1s spectra (Fig. 8a). Both correspond to the formation of O–C=O and C–O functional groups, respectively, indicative of the oxidation of AG MP-50 backbone.[39] In line with previous research, the main mechanism of this oxidation is an indirect radiolysis, caused by free radicals (*e.g.*, hydroxyl radicals and hydrogen peroxide), which primarily originate from the interaction between the gamma rays and the solution.[40] Deconvolution of the spectra leads to a quantification of ~2.3 at% of carboxylic species at the surface of the sample, which received 11 MGy dose (Table 1). The normalized O 1s (Fig. 8b) and S 2p (Fig. 8c) did not show apparent changes as the absorbed dose increased. The interpretation reveals that the surface sulfur content of AG MP-50 decreased from approximately 6.5 at% to 4.5 at% after receiving a dose of 11 MGy. Moreover, no marked differences were detected in terms of surface oxygen and sulfur content for the pristine and irradiated AG MP-50 with an absorbed dose of 1 MGy, possibly due to limitations of the XPS technique and the possibility of measurement errors. When the absorbed dose increased up to 11 MGy, the surface oxygen content of the irradiated AG MP-50 slightly decreased from approximately 22 at% to 20 at%. These outcomes can be explained by radiation-induced decomposition of the sulfonic acid groups due to the high levels of gamma-ray irradiation.[8]

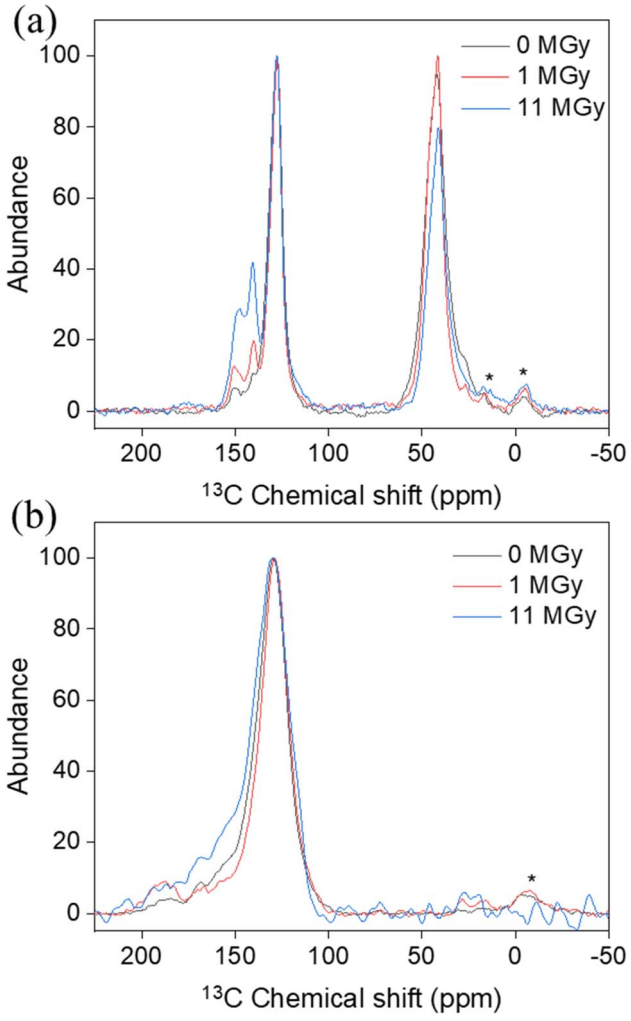

Fig. 7 ^{13}C-CPMAS NMR spectra of the pristine and irradiated AG MP-50 (a) and SAC (b).

3.2.2. Sulfonated activated carbon. The DRIFT spectra (as shown in Fig. 6b) exhibited distinct bands at approximately 1710 and 1220 cm^{-1}, which are associated with the stretching of C=O and C–O bonds, respectively.[41–45] Additionally, the band at 1000–1070 cm^{-1} is indicative of the S=O stretching vibration.[41–45] The stretching vibration of the aromatic C=C bonds is assigned to the band located at 1600 cm^{-1}, whereas the bands at around 896 and 830 cm^{-1} are assigned to the out-of-plane bending vibrations of C–H in the aromatic rings.[37] Notably, there were no apparent changes in these DRIFT bands for SAC materials before and after exposure to gamma irradiation. These outcomes indicate that the species of the functional groups were still present. In addition, the NMR (Fig. 7b) and XPS (Fig. 8d–f) spectra provide further information on the functional groups. The signal around 130 ppm in the NMR spectra can be attributed to polycyclic aromatic carbon atoms.[46,47] After exposure to an absorbed dose of 1 MGy, the phenolic OH of SAC oxidized to aldehyde as the phenolic C–OH signal at around 155 ppm of decreased and a clear aldehyde signal around 190 ppm appears. When the absorbed dose reaches 11 MGy, further oxidation of aldehyde (~190 ppm) to carboxylic acid (~170 ppm) appears to occur, leading to a decrease in signal around 190 ppm while a signal is formed around 170 ppm.[46,47] Also, the intensity around 155 ppm increases again, probably due to some oxidation of aromatic carbons to phenolic C–OH carbons. The bandwidth of the SAC signals also increases slightly with increasing absorbed dose, indicating radiation-induced oxidation and the formation of

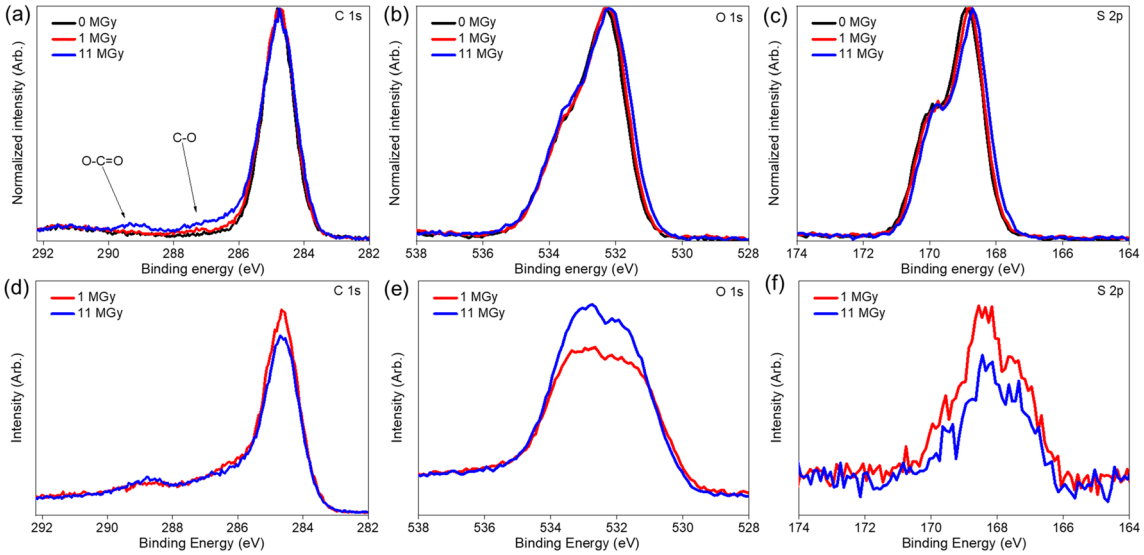

Fig. 8 High-resolution XPS curves of C 1s (a), O 1s (b), and S 2p (c) of the pristine and irradiated AG MP-50 resins, and high-resolution XPS curves of C 1s (d), O 1s (e), and S 2p (f) of the irradiated SAC.

multiple, slightly different environments for the carbons. As demonstrated in Fig. S2c and d,† the C 1s high-resolution spectra of the pristine (earlier work[19]) and irradiated SAC exhibited six binding energies, representing the existence of C–C/C=C, C–N/C–O/C–S, C=O, O–C=O and CO_3 environments and a $\pi^* \leftarrow \pi$ satellite peak.[39] The O 1s high-resolution spectra (Fig. S2a and b†) exhibited three binding energies, representing the manifestation of O=C/O=S and O–C/O–S environments and a $\pi^* \leftarrow \pi$ satellite peak. The presence of the oxidized sulfur-containing groups was also confirmed by the S 2p high-resolution XPS spectra (Fig. S2e and f†). These results clearly indicate that the carbonyl, carboxylic, and oxidized sulfur-containing groups were still present on the surface. Although there was no change in the species of the functional groups, the quantitative interpretation of the XPS analysis showed that the content of the different types of functional groups changed. The surface O/C molar ratio (Table 1) increased with increasing adsorbed dose from 0.17 (0–1 MGy) to 0.21 (11 MGy), indicating that oxygen-containing groups were grafted on the surface of irradiated SAC at a dose of 11 MGy. In addition, the collected C 1s high-resolution spectra show a minor increase in the intensity of the O–C=O peaks (Fig. 8d). The percentage composition of O atoms increased from approximately 14 at% to 17 at% when SAC received a dose of 11 MGy (Table 1), which was primarily attributed to the increase of carboxylic groups from approximately 2.7 at% to 4.5 at%. This effect occurred because some functional groups or carbon structures were oxidized by free radicals, as illustrated above. Compared with the oxygen-containing groups, the content of the oxidized sulfur-containing groups also decreased from approximately 0.9 at% to 0.5 at% due to radiolytic decomposition of the oxidized sulfur-containing groups. These results imply that the carboxylic acid groups on the surface of the carbon structure were less susceptible to radiolytic damage than the sulfur-containing groups.

3.3. Effect of gamma irradiation on sorption performance

The sorption performance of the pristine and irradiated sorbents is regarded as a vital indicator for tracking the impact of the radiolysis to the sorbents.[4,18] In this study, La^{3+} was utilized as a non-radioactive surrogate for $^{225}Ac^{3+}$, as demonstrated in our earlier work.[19] It should be noted that although non-radionuclide La^{3+} and Bi^{3+} are expected to exhibit similar chemical behaviors as $^{225}Ac^{3+}$ and $^{213}Bi^{3+}$, the use of stable metals as analogs presents certain drawbacks. Specifically, experiments with micrograms of stable La^{3+} and Bi^{3+} might not reveal the effects of impurities, which otherwise could substantially impact experiments or applications involving $^{225}Ac^{3+}$ and $^{213}Bi^{3+}$ separation typically present in significantly lower quantity.

The sorption mechanism of AG MP-50 for $La^{3+}(Ac^{3+})/Bi^{3+}$ is attributed to the electrostatic attraction or ion exchange between the sulfonic acid groups and the metal ions.[20] The sorption experiments were designed to investigate the decrease in concentration or number of sulfonic acid groups rather than its optimal sorption performance. Hence, a highly acidic solution (1.5 mol L^{-1} HNO_3) was selected to avoid any interference of the carboxylic groups with a relatively high pK_a value (usually >2).[20] Therefore, only sulfonic acid groups were presumed to be the active sorption sites for La^{3+} during the sorption process. Fig. 9a illustrates that the K_d values and sorption percentages for La^{3+} sorption onto the pristine and irradiated AG MP-50 resins decreased significantly with increasing the absorbed dose, especially at a dose of 11 MGy. Additionally, the sorption performance of AG MP-50 towards Bi^{3+} decreased with increasing absorbed dose. These results clearly indicate that the active sorption sites decreased as a result of the gamma irradiation, which is probably attributed to the decomposition of sulfonic acid groups and the aggregation of AG MP-50 particles. The decrease in sorption capacity at high absorbed doses is

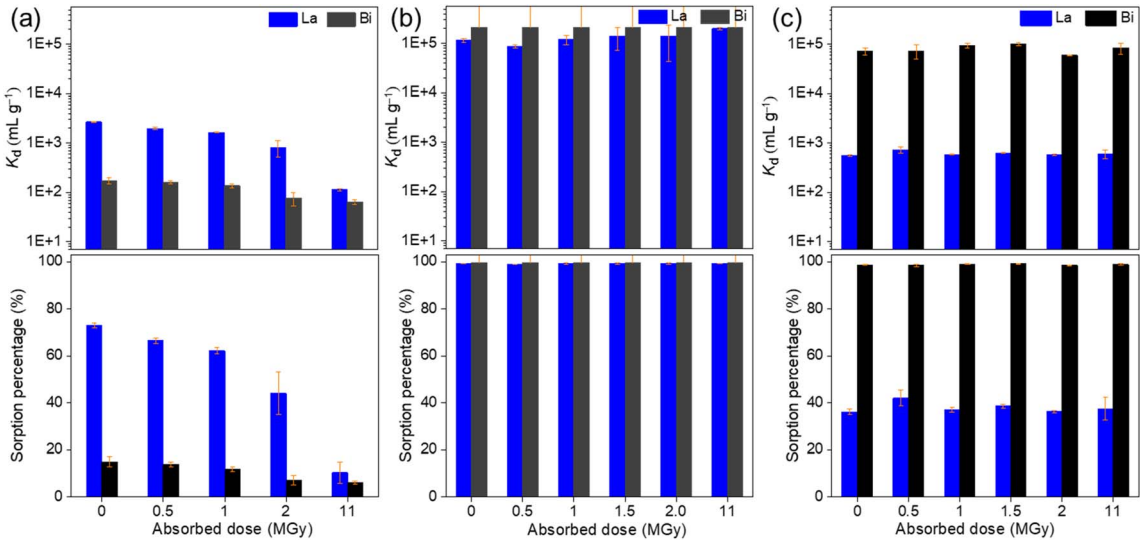

Fig. 9 Sorption performance of La^{3+}/Bi^{3+} sorption onto the pristine and irradiated AG MP-50 resins at 1.5 mol L^{-1} HNO_3 (a), and the pristine and irradiated SAC at pH = 2 (b) and pH = 1 (c). (C_0 (La^{3+}) = 10 μmol L^{-1}, C_0 (Bi^{3+}) = 10 μmol L^{-1}, S: L = 1 g L^{-1}, t = 24 h, binary system) (data of SAC at 0 and 1 MGy are from our previous paper[19]).

most likely to impact the breakthrough of adsorbed ^{225}Ac. Furthermore, the formation of oxygen-containing groups could affect the ^{213}Bi yield, as Bi^{3+} has a high affinity for oxygen-containing groups. Alterations in the morphology may also affect the ^{213}Bi yield.

Fig. 9b and c display the sorption performance of the pristine and irradiated SAC materials towards La^{3+}/Bi^{3+} as a function of absorbed dose at pH = 2 and pH = 1, respectively. More specifically, at pH = 2, the equilibration concentration of Bi^{3+} was less than 10 μg L^{-1}, which corresponds to a K_d value of more than 10^5 mL g^{-1}. The K_d values for La^{3+} were of similar magnitude, and there was no statistically significant reduction with increasing radiation dose. At pH = 1, no significant changes in La^{3+}/Bi^{3+} sorption were observed. In particular, the K_d values for Bi^{3+} were higher than 10^4 mL g^{-1}, indicating that the SAC could be used for separating Bi^{3+} in the sorption process of inverse generators, even after receiving a gamma dose of 11 MGy. It can be argued that the Bi^{3+} and La^{3+} sorption was not highly sensitive to gamma-ray irradiation doses below 11 MGy. This phenomenon could be attributed to the simultaneous effects of the cleavage and oxidation of functional groups and the formation of new ones throughout the irradiation process.

3.4. Application of AG MP-50 and SAC in ^{225}Ac/^{213}Bi generators

AG MP-50 resin is commonly utilized as a sorbent in direct ^{225}Ac/^{213}Bi generators, as well as in the guard or accumulation column for further purification and concentration of ^{213}Bi. The sorption performance of SAC and their high radiolytic stability, as demonstrated in this study, make it a promising candidate for use in inverse ^{225}Ac/^{213}Bi generators as an alternative to UTEVA. Herein, the operation conditions of AG MP-50 resin and SAC for the ^{225}Ac and ^{213}Bi separation were discussed regarding their radiolytic stability and received doses. It is also well-established that the absorbed dose of the sorbents is closely related to their mass and the irradiation conditions. Specifically, an increase in the mass of the sorbents results in a lower absorbed dose when receiving the same energy. Here, the absorbed dose D (in J kg^{-1} = Gy) of the sorbents was calculated by using the following equation:[4]

$$D = 1.602 \times 10^{-10} \times A_0 \frac{1 - e^{-\lambda t}}{\lambda} \times \frac{Q_\alpha}{m} \quad (3)$$

where m (g) represents the mass of the material in the column that is contacted with radionuclides, Q_α represents the sum of all α-particles energies (in MeV) in the decay chain of ^{225}Ac, including its descendants ^{221}Fr, ^{217}At, ^{213}Bi, and ^{213}Po.[48] A_0 (Bq) is the initial activity of ^{225}Ac and 4 GBq ^{225}Ac was chosen as the starting activity with Q_α being about 28 MeV, and assuming radioactive equilibrium (λ = 8.09 × 10^{-7} s^{-1}).[7,48] The received dose of the sorbents as a function of contact time was calculated and is presented in Fig. 10.

Based on the batch sorption results in Fig. 9 and our earlier work, 10 mg of AG MP-50 resin was sufficient to adsorb 8.3 nmol of ^{225}Ac, corresponding to 4 GBq.[19] However, this result indicates that the AG MP-50 is likely to be destroyed within a short period of time (less than a few hours) due to the absorbed dose reaching 11 MGy within 2 hours (Fig. 10). As a result, various efforts have been focused on increasing the contact area of radionuclides on a larger mass of sorbent to effectively reduce its absorbed dose.[5] This could be achieved by decreasing the sorption capacity of AG MP-50 for ^{225}Ac by increasing the acid concentration or adding an excess of its surrogate La^{3+} for the occupation of the active sorption sites.[5,49] Although these methods are beneficial in reducing radiolytic damage, using a larger mass of AG MP-50 in the column could possibly result in reduced activity of ^{213}Bi due to the increased diffusion path

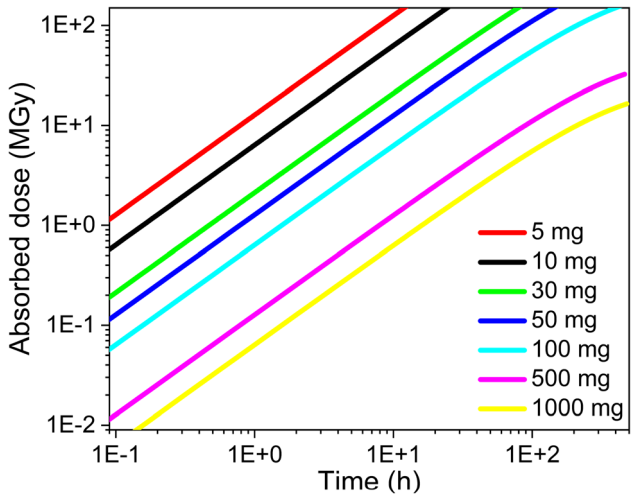

Fig. 10 Absorbed dose of the sorbent as a function of the contact time.

lengths. Additionally, even in the case where the mass of AG MP-50 is 1 g, this generator does not seem to operate satisfactorily for more than one week (Fig. 10). With a half-life of 9.920 days, a significant amount of ^{225}Ac (>60%) would still be present on such a generator.

Radiation stability is a crucial factor influencing the shelf-life of sorbents in radionuclide generators. An earlier review has summarized the radiation stability of several materials, including AG 50 W-X8, Dowex 50-X4, Actinide and UTEVA resins.[4] Generally, resins with high cross-linkages demonstrate greater radiation stability compared to those with low cross-linkage structures. In addition, extraction chromatographic resins show lower radiation stability compare to ion exchange resins due to the instability and leaching of their extractants.

Compared to previously reported sorbents that have been used for the inverse ^{225}Ac/^{213}Bi radionuclide generators, the SAC is chemically more stable under strongly acidic conditions (pH < 2) than inorganic metal oxides (*e.g.*, Termoxid-39) and has higher radiolytic stability compared to organic resins (*e.g.*, UTEVA resin).[4] However, the shape and particle size of such types of materials are important influencing factors. Therefore, using spherically-shaped SAC material with appropriate particle sizes would be a favorable choice.

4. Conclusions

The radiolytic stability of the AG MP-50 cation exchange resin and sulfonated activated carbon (SAC) was systematically evaluated by combining material characterization techniques (SEM, XRD, FT-IR, solid-state NMR, and XPS) and sorption tests. The irradiated AG MP-50 resin and SAC material with absorbed doses ranging from 0.5 to 11 MGy were obtained by exposing samples to ^{60}Co radiation. The polymeric particle structures of AG MP-50 resin changed on exposure to 11 MGy, as observed by solid-state NMR and the occurrence of color changes, scission of polymeric chains, and particle aggregation. The decrease in the number of the surface sulfonic acid groups and the particle aggregation for the irradiated AG MP-50 resins resulted in a significant reduction in the sorption performance towards La^{3+}. Furthermore, carboxylic groups also formed due to free radical-induced oxidation. It was revealed that the AG MP-50 resin exhibited a higher sensitivity to irradiation compared to the investigated SAC materials. In contrast, no apparent changes in the morphology of the irradiated SAC materials were detected, even at a high absorbed dose of 11 MGy. Similar to AG MP-50, the SAC structures were also oxidized by free radicals, corresponding to an increase in the content of the carboxylic groups. Despite these changes, the sorption capacity of the irradiated SAC materials towards La^{3+}/Bi^{3+} remained stable, implying that there was no significant reduction in the number of active sorption sites. Additionally, the absorbed dose of such materials in the inverse generators is relatively low due to the short contact time between the radionuclides and the sorbents. Therefore, SAC can be applied for the separation of large-scale ^{213}Bi (*e.g.*, 4 GBq) production. The low radiolytic resistance of AG MP-50 limits its application for separating ^{213}Bi in direct generators. These findings provide valuable insights for understanding the radiolytic effects on AG MP-50 and SAC that can be used in ^{225}Ac/^{213}Bi radionuclide generators.

Author contributions

Hongshan Zhu: conceptualisation, data curation, formal analysis, investigation, methodology, validation, visualisation, writing – original draft. Stephan Heinitz: conceptualisation, formal analysis, investigation, methodology, visualisation, writing – review & editing, funding acquisition. Samuel Eyley: data curation, formal analysis, investigation, writing – review & editing. Wim Thielemans: investigation, writing – review & editing, funding acquisition. Elien Derveaux: investigation, writing – review & editing. Peter Adriaensens: investigation, writing – review & editing, funding acquisition. Koen Binnemans: conceptualisation, supervision, formal analysis, investigation, methodology, visualisation, writing – review & editing, funding acquisition. Steven Mullens: conceptualisation, formal analysis, investigation, methodology, visualisation, writing – review & editing, funding acquisition. Thomas Cardinaels: conceptualisation, supervision, formal analysis, investigation, methodology, visualisation, writing – review & editing, funding acquisition.

Conflicts of interest

There are no conflicts to declare.

Acknowledgements

The SCK CEN Academy and VITO are acknowledged for funding. Samuel Eyley and Wim Thielemans also acknowledge financial support from KU Leuven (grant C14/18/061) and Research Foundation Flanders-FWO (G0A1219N). Peter Adriaensens gratefully acknowledges the financial support by Hasselt University and the Research Foundation Flanders (FWO Vlaanderen) *via* the Hercules project AUHL/15/2-GOH3816N.

Furthermore, the authors would like to acknowledge the technical assistance of Prisca Verheyen (ICP-MS), Ken Verguts (material irradiation), Myrjam Mertens (XRD), Hilde Lenaerts & Kaimin Zhang & Vera Meynen (DRIFT), and Kemps Raymond (SEM).

References

1 A. Dash and R. Chakravarty, Pivotal role of separation chemistry in the development of radionuclide generators to meet clinical demands, *RSC Adv.*, 2014, **4**, 42779–42803.
2 S. Ermolaev, A. Skasyrskaya and A. Vasiliev, A Radionuclide Generator of High-Purity Bi-213 for Instant Labeling, *Pharmaceutics*, 2021, **13**, 914.
3 T. I. Kostelnik and C. Orvig, Radioactive Main Group and Rare Earth Metals for Imaging and Therapy, *Chem. Rev.*, 2018, **119**, 902–956.
4 A. N. Vasiliev, V. A. Zobnin, Y. S. Pavlov and V. M. Chudakov, Radiation Stability of Sorbents in Medical ^{225}Ac/^{213}Bi Generators, *Solvent Extr, Ion Exch.*, 2021, **39**, 353–372.
5 M. R. McDevitt, R. D. Finn, G. Sgouros, D. Ma and D. A. Scheinberg, An ^{225}Ac/^{213}Bi generator system for therapeutic clinical applications: construction and operation, *Appl. Radiat. Isot.*, 1999, **50**, 895–904.
6 D. R. McAlister and E. Philip Horwitz, Automated two column generator systems for medical radionuclides, *Appl. Radiat. Isot.*, 2009, **67**, 1985–1991.
7 A. Morgenstern, C. Apostolidis and F. Bruchertseifer, Supply and Clinical Application of Actinium-225 and Bismuth-213, *Semin. Nucl. Med.*, 2020, **50**, 119–123.
8 K. K. S. Pillay, A review of the radiation stability of ion exchange materials, *J. Radioanal. Nucl. Chem.*, 1986, **102**, 247–268.
9 T. E. Gangwer, M. Goldstein and K. K. S. Pillay, *Radiation Effects on Ion Exchange Materials*, United States, 1977, BNL 50781, **https://www.osti.gov/servlets/purl/6548668**.
10 M. F. McLaughlin, J. Woodward, R. A. Boll, A. J. Rondinone, S. Mirzadeh and J. D. Robertson, Gold-coated lanthanide phosphate nanoparticles for an ^{225}Ac in vivo alpha generator, *Radiochim. Acta*, 2013, **101**, 595–600.
11 A. K. H. Robertson, C. F. Ramogida, C. Rodríguez-Rodríguez, S. Blinder, P. Kunz, V. Sossi and P. Schaffer, Multi-isotope SPECT imaging of the ^{225}Ac decay chain: feasibility studies, *Phys. Med. Biol.*, 2017, **62**, 4406–4420.
12 G. Ardisson, V. Barci and O. El Samad, Nuclear levels and structure from the decays of ^{213}Bi and ^{209}Tl, *Phys. Rev. C*, 1998, **57**, 612–620.
13 D. Kleut, S. Jovanović, Z. Marković, D. Kepić, D. Tošić, N. Romčević, M. Marinović-Cincović, M. Dramićanin, I. Holclajtner-Antunović, V. Pavlović, G. Dražić, M. Milosavljević and B. Todorović Marković, Comparison of structural properties of pristine and gamma irradiated single-wall carbon nanotubes: Effects of medium and irradiation dose, *Mater. Charact.*, 2012, **72**, 37–45.
14 G. Bond, H. Eccles and J. D. Emmott, The Acid and Radiation Stability of Some Commercial Ion Exchangers, *J. Chem. Eng. Process Technol.*, 2019, **10**, 394, DOI: **10.35248/2157-7048.19.10.394**.
15 S. F. Marsh and K. K. S. Pillay, *Effects of ionizing radiation on modern ion exchange materials*, Los Alamos National Lab., United States, 1993, LA-12655-MS.
16 D. Ma, M. R. McDevitt, R. D. Finn and D. A. Scheinberg, Breakthrough of ^{225}Ac and its radionuclide daughters from an ^{225}Ac/^{213}Bi generator: development of new methods, quantitative characterization, and implications for clinical use, *Appl. Radiat. Isot.*, 2001, **55**, 667–678.
17 C. Wu, M. W. Brechbiel and O. A. Gansow, An improved generator for the production of ^{213}Bi from ^{225}Ac, *Radiochim. Acta*, 1997, **79**, 141–144.
18 A. R. Kazanjian and M. E. Killion, *Radiation Effects on Amberlite IRA-938 and Bio-rad AG MP-50 Ion Exchange Resins*, Rockwell International Corp., Rocky Flats Plant., Golden, United States, 1982, RFP-3167, DOI: **10.2172/5552116**.
19 H. Zhu, S. Heinitz, S. Eyley, W. Thielemans, K. Binnemans, S. Mullens and T. Cardinaels, Sorption and desorption performance of La^{3+}/Bi^{3+} by surface-modified activated carbon for potential application in medical ^{225}Ac/^{213}Bi generators, *Chem. Eng. J.*, 2023, **464**, 142456.
20 V. Beaugeard, J. Muller, A. Graillot, X. Ding, J. J. Robin and S. Monge, Acidic polymeric sorbents for the removal of metallic pollution in water: A review, *React. Funct. Polym.*, 2020, **152**, 104599.
21 E. Mansouri, A. Mesbahi, R. Malekzadeh and A. Mansouri, Shielding characteristics of nanocomposites for protection against X- and gamma rays in medical applications: effect of particle size, photon energy and nano-particle concentration, *Radiat. Environ. Biophys.*, 2020, **59**, 583–600.
22 A. R. Kazanjian and D. R. Horrell, *Radiation effects on ion-exchange resins, Part III, Alpha irradiation of Dowex 50W*, Rocky Flats Division, Golden, Colorado, United States, 1975, RFP-2354, DOI: **10.2172/4215563**.
23 A. R. Kazanjian and D. R. Horrell, *Radiation effects on ion exchange resins. I. Gamma irradiation of Dowex 50W*, Rocky Flats Division, Golden, Colorado, United States, 1974, RFP-2140, DOI: **10.2172/4297685**.
24 A. Ashfaq, M. C. Clochard, X. Coqueret, C. Dispenza, M. S. Driscoll, P. Ulanski and M. Al-Sheikhly, Polymerization Reactions and Modifications of Polymers by Ionizing Radiation, *Polymers*, 2020, **12**, 2877.
25 A. T. Naikwadi, B. K. Sharma, K. D. Bhatt and P. A. Mahanwar, Gamma Radiation Processed Polymeric Materials for High Performance Applications: A Review, *Front. Chem.*, 2022, **10**, 837111.
26 T. Kwamman, S. Anantachaisilp, P. Limmeechokchai and K. Kanjana, Enhancements of surface functional groups and degree of graphitization in gamma irradiated activated carbon as an electrode material, *Radiat. Phys. Chem.*, 2022, **195**, 110062.
27 H. Zhu, S. Heinitz, S. Eyley, W. Thielemans, K. Binnemans, S. Mullens and T. Cardinaels, Selective separation of Bi^{3+} from La^{3+}/Ac^{3+} by sorption on sulfonated carbon materials

for use in an inverse $^{225}Ac/^{213}Bi$ radionuclide generator: Batch and column tests, *Chem. Eng. J.*, 2023, **468**, 143416.
28 B. Verlinden, P. Zsabka, K. Van Hecke, K. Verguts, L. C. Mihailescu, G. Modolo, M. Verwerft, K. Binnemans and T. Cardinaels, Dosimetry and methodology of gamma irradiation for degradation studies on solvent extraction systems, *Radiochim. Acta*, 2021, **109**, 61–72.
29 R. Li, Y. Gu, Z. Yang, M. Li, S. Wang and Z. Zhang, Effect of γ irradiation on the properties of basalt fiber reinforced epoxy resin matrix composite, *J. Nucl. Mater.*, 2015, **466**, 100–107.
30 A. M. Dessouki, A. H. Zahran, A. M. Rabie and S. I. Amer, Some investigations on the radiation stability of a strongly acidic cation exchange resin, *Radiat. Phys. Chem.*, 1989, **33**, 545–549.
31 G. M. Vinhas, R. M. Souto Maior and Y. M. B. Almeida, Radiolytic degradation and stabilization of poly(vinyl chloride), *Polym. Degrad. Stab.*, 2004, **83**, 429–433.
32 G. G. Flores-Rojas, F. López-Saucedo and E. Bucio, Gamma-irradiation applied in the synthesis of metallic and organic nanoparticles: A short review, *Radiat. Phys. Chem.*, 2020, **169**, 107962.
33 C. Huang, K. Seng Tan, J. Lin and K. Lee Tan, XRD and XPS analysis of the degradation of the polymer electrolyte in H_2–O_2 fuel cell, *Chem. Phys. Lett.*, 2003, **371**, 80–85.
34 B. Li, D. Huang, T. Li, C. Ye, N. Zhang, X. Zhou, Z. Fan, G. Liao, F. Han, H. Liu and J. Liu, The positive role of mesophase-pitch-based carbon fibers in enhancing thermal response behavior in Carbon/Carbon composites, *Mater. Charact.*, 2023, **196**, 112630.
35 B. Li, Y. Feng, K. Ding, G. Qian, X. Zhang and J. Zhang, The effect of gamma ray irradiation on the structure of graphite and multi-walled carbon nanotubes, *Carbon*, 2013, **60**, 186–192.
36 B. Li, Y. Feng, G. Qian, J. Zhang, Z. Zhuang and X. Wang, The effect of gamma ray irradiation on PAN-based intermediate modulus carbon fibers, *J. Nucl. Mater.*, 2013, **443**, 26–31.
37 S. Ghosh, K. Dhole, M. K. Tripathy, R. Kumar and R. S. Sharma, FTIR spectroscopy in the characterization of the mixture of nuclear grade cation and anion exchange resins, *J. Radioanal. Nucl. Chem.*, 2015, **304**, 917–923.
38 L. Kong, Y. Cheng, Y. Jin, T. Qi and F. Xiao, Low *k* epoxy resin containing cycloaliphatic hydrocarbon with high crosslinking density, *J. Appl. Polym. Sci.*, 2016, **133**, 43456.
39 X. Chen, X. Wang and D. Fang, A review on C1s XPS-spectra for some kinds of carbon materials, *Fullerenes, Nanotubes Carbon Nanostruct.*, 2020, **28**, 1048–1058.
40 I. Velo-Gala, J. J. López-Peñalver, M. Sánchez-Polo and J. Rivera-Utrilla, Surface modifications of activated carbon by gamma irradiation, *Carbon*, 2014, **67**, 236–249.
41 I. Ogino, Y. Suzuki and S. R. Mukai, Tuning the Pore Structure and Surface Properties of Carbon-Based Acid Catalysts for Liquid-Phase Reactions, *ACS Catal.*, 2015, **5**, 4951–4958.
42 Q. Xu, Z. Yang, D. Yin and F. Zhang, Synthesis of chalcones catalyzed by a novel solid sulfonic acid from bamboo, *Catal. Commun.*, 2008, **9**, 1579–1582.
43 N. Duyckaerts, I. T. Trotuș, V. Nese, A. C. Swertz, S. Auris, H. Wiggers and F. Schüth, Mesoporous Sulfonated Carbon Materials Prepared by Spray Pyrolysis, *ChemCatChem*, 2015, **7**, 2891–2896.
44 S. Dutta, A. Bohre, W. Zheng, G. R. Jenness, M. Núñez, B. Saha and D. G. Vlachos, Solventless C–C Coupling of Low Carbon Furanics to High Carbon Fuel Precursors Using an Improved Graphene Oxide Carbocatalyst, *ACS Catal.*, 2017, **7**, 3905–3915.
45 R. Zhong, Y. Liao, R. Shu, L. Ma and B. F. Sels, Vapor-phase assisted hydrothermal carbon from sucrose and its application in acid catalysis, *Green Chem.*, 2018, **20**, 1345–1353.
46 K. Nakajima and M. Hara, Amorphous Carbon with SO_3H Groups as a Solid Brønsted Acid Catalyst, *ACS Catal.*, 2012, **2**, 1296–1304.
47 M. Okamura, A. Takagaki, M. Toda, J. N. Kondo, K. Domen, T. Tatsumi, M. Hara and S. Hayashi, Acid-Catalyzed Reactions on Flexible Polycyclic Aromatic Carbon in Amorphous Carbon, *Chem. Mater.*, 2006, **18**, 3039–3045.
48 S. Ahenkorah, I. Cassells, C. M. Deroose, T. Cardinaels, A. R. Burgoyne, G. Bormans, M. Ooms and F. Cleeren, Bismuth-213 for Targeted Radionuclide Therapy: From Atom to Bedside, *Pharmaceutics*, 2021, **13**, 599.
49 A. Christos, B. Brandalise, R. Carlos-Marquez, W. Janssens, R. Molinet and T. Nikula, Method of loading a radioelement generator with mother radionuclide, *US Pat.*, US2005/0008553, 2005.